Design and Performance Analysis of Permanent Magnet Claw Pole Machine with Hybrid Cores

Chengcheng Liu, *Member, IEEE*, Zheng Chao, Shaopeng Wang, and Youhua Wang

***Abstract*—Permanent magnet claw pole machine (PMCPM) is a special kind of transverse flux permanent magnet machine. Compared with other electrical machines, it has the advantages of high torque density and high efficiency for high speed operation. However, because of its complex irregular structure, the manufacturing process using silicon sheets is complicated. Soft magnetic composite material (SMC) is manufactured by powder metallurgy technology, which can produce various shapes of stator core structures, so it is easier to produce various irregular shapes of the stator core. However, the raw SMC material is relatively expensive, and the mechanical strength of SMC is weak. In this paper, a PMCPM with hybrid cores is proposed. With the adoption of hybrid silicon sheet - SMC cores and amorphous alloy - SMC cores, the torque ability of PMCPM can be improved greatly and it can have higher efficiency for more wide operation frequency. Meanwhile, its mechanical strength has been improved and it can be designed for high torque direct drive applications as it is a modular machine. Furthermore, three methods are proposed to reduce the additional eddy current loss which resulted from the employment of hybrid cores in PMCPM.**

***Index Terms*—Permanent magnet claw pole machine (PMCPM), Soft magnetic materials (SMC), Hybrid cores, Eddy current loss.**

I. Introduction

With adoption of global winding and 3-D magnetic flux structure, the permanent magnet claw-pole machine (PMCPM) can exhibit higher torque ability than other types of electrical machines [1]-[3]. However, it is very difficult to develop PMCPM with traditional silicon sheets, as its main magnetic flux structure is very complex. The soft magnetic composite (SMC) is a relative new kind of soft magnetic material which made by iron powder surrounded by insulation layer [4]. Based on powder metallurgical technology, developing PMCPM with SMC cores will be quite simple. In the past decades, many works have been done on developing, analyzing and design optimization of PMCPM with SMC cores (SMC-CPM) [5]-[7].

Compared with silicon sheets, the SMC has the advantages of low eddy current loss and magnetic isotropic characteristic [8]-[9], while its disadvantages include low permeability, low mechanical strength and even high cost of raw material due to the production scale of SMC powder is very small currently [10]. In the design of electrical machine with SMC cores, some design guidelines were suggested to be followed, e.g., PM excitation, 3D magnetic flux structure, and high operation frequency. Currently, the SMC-CPM is normally designed with small size, as the heat treatment process for dealing large SMC cores is very complex moreover the large compaction machine is required for punching large SMC core. Meanwhile, the mechanical strength of the claw pole teeth made by SMC is relatively low, which makes the robustness of SMC-CPM is not high. To overcome above constraints, developing PMCPM with hybrid cores (Hybrid-CPM) is an effective way [11]-[13].

Amorphous alloy (AAM) is a relatively new soft magnetic material. Compared with silicon sheets, it has the advantages of high permeability, low core loss characteristic, and high resistivity [14]. It is an ideal soft magnetic material for developing high efficiency electrical machines and transformers. Compared with the PM machines based on silicon sheets, the core loss of PM machine with amorphous alloy is much lower [15]-[16].

Based on these soft magnetic materials and machine topology, this paper proposes a PMCPM with hybrid silicon sheet and SMC cores (Si-SMC-CPM) and a PMCPM with hybrid amorphous alloy and SMC cores (AAM-SMC-CPM). The proposed machines can have following merits. Firstly, the cost can be reduced as some part will be replaced by silicon sheets or amorphous alloy. Secondly, the operation frequency of the proposed machine can be designed not too much high thus the system can be used for more applications. Thirdly, the torque ability of PMCPM can be improved. Lastly, this machine has the potential to be designed with large size that used for wind generator and electric vehicle drive system. On the other hand, with the employment of hybrid cores, the additional eddy current loss will be resulted on the joint part of hybrid core which will decrease the efficiency of PMCPM with hybrid cores. In this paper, its reduction methods are investigated in the last section.

In this paper, the section II compares the magnetic characteristics of different materials, including silicon steels,

Manuscript received September 09, 2022; revised October 31, 2022, and December 07, 2022; accepted December 21, 2022. Date of publication September 25, 2023; date of current version March 04, 2023.

This work was supported by the National Natural Science Foundation of China under project 52007047, and in part by the Outstanding Youth Innovation Project funded by State Key Laboratory of Reliability and Intelligence of Electrical Equipment EERI_OY2021005.

Chengcheng Liu, Zheng Chao, Shaopeng Wang, and Youhua Wang are with State Key Laboratory of Reliability and Intelligence of Electrical Equipment, Hebei University of Technology and Key Laboratory of Electromagnetic Field and Electrical Apparatus Reliability of Hebei Province, Hebei University of Technology, Tianjin 300130, China (2016020@hebut.edu.cn, 1144659033@qq.com, 522396000@qq.com, wangyi@hebut.edu.cn).

(Corresponding Author: Chengcheng Liu)

Digital Object Identifier 10.30941/CESTEMS.2023.00027

SMC and amorphous alloys, and then describes the structures of SMC-CPM and the proposed Hybrid-CPM. In the section Ⅲ, the main structural parameters of SMC-CPM and Hybrid-CPM are determined. On this basis, the basic electromagnetic characteristics and performances of SMC-CPM, Si-SMC-CPM and Alloy-SMC-CPM are analyzed. The last section analyzes the distribution of the additional eddy current loss at the joint of the hybrid core and corresponding additional eddy current loss reduction methods are analyzed.

II. Main Magnetic Topology of PMCPM with Hybrid Cores

A. Magnetic Characteristic Comparison among SMC, Silicon Sheet and Amorphous Alloy

Fig. 1 shows the BH curve comparison of SMC, amorphous alloy, and silicon sheet, it can be seen that the permeability of silicon sheet and amorphous alloy is much higher than that of SMC. Fig. 2 shows the core loss versus the magnetic flux density under different operation frequency comparison of SMC, amorphous alloy and silicon sheets. Table I tabulates the main characteristic of these materials. Due to the special manufacturing process of amorphous alloy, its coercive force is much lower than that of SMC and silicon sheets, therefore its hysteresis loss is very low. On the other hand, the saturation flux density of amorphous alloy is lower than that of other two materials. Therefore, in the design of electrical machine with amorphous alloy the maximum operation flux density needs to be lower than 1.5 T. For the SMC material, its advantages including the magnetic isotropic and low eddy current loss. In the design of electrical machines, above materials have their own merits. Considering the flux distribution characteristic in the electrical machine and the different material properties, the performance of electrical machine can be improved by employing the suitable material for designing different part of the machine.

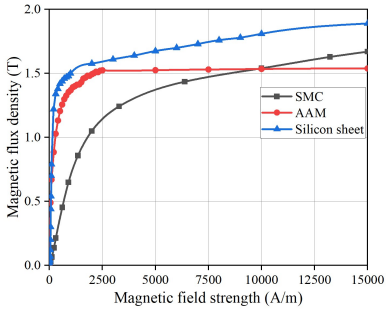

Fig. 1. BH curve of SMC, amorphous alloy and silicon sheet.

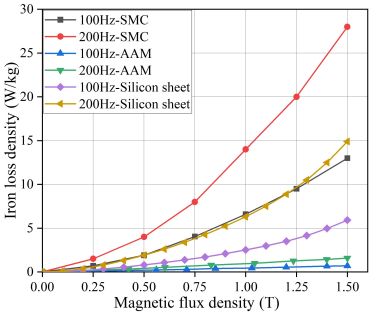

Fig. 2. Core loss characteristic of SMC, amorphous alloy and silicon sheet.

TABLE I
CHARACTERISTICS COMPARISON OF DIFFERENT MATERIALS

	SMC	AAM	Silicon sheet
Coercivity(A/m)	120	4	30
Vickers hardness (Hv)	160	900	181
Density(g/cm^3)	7.5	7.18	7.65
Resistivity (μΩ/m)	700	1.3	0.45

B. Topology of SMC-CPM

Fig. 3(a) shows the main magnetic structure of SMC-CPM. For simplicity, only one of the three stacks is plotted. The complete machine has three stacks with the stator cores shifted by 120° (electrical) from each other and the rotor stacks aligned. The rotor is made by using silicon sheets, and the NdfeB permanent magnets (PMs) are mounted on the surface of the rotor core. For reducing cogging torque and torque ripple, the stator claw pole teeth are designed with unequal width structure. Fig. 3(b) shows the no load flux density vector of the PMCPM. On this basis, the main magnetic flux path in the PMCPM is shown in Fig. 3(c). As shown, the magnetic flux path length of stator core made by SMC occupies a great ratio of total magnetic circuit length, therefore the magnetic characteristic of SMC determines the performance of SMC-CPM.

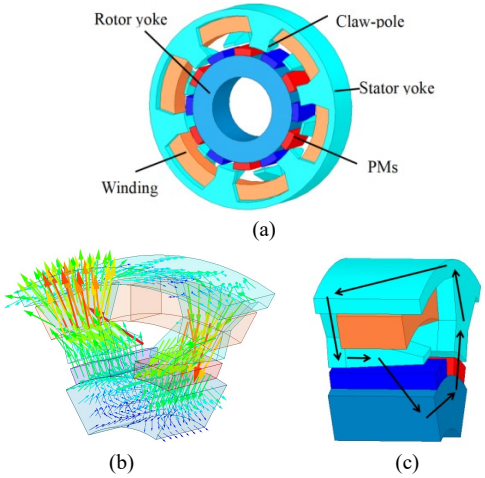

Fig. 3. (a) Schematic diagram of the topology of SMC-CPM. (b) flux line distribution of PMCPM. (c) main magnetic circuit of PMCPM.

C. Main Topology of Hybrid-CPM

Fig. 4(a) shows the main magnetic structure of PMCPM with hybrid SMC and silicon sheet or amorphous alloy cores. Due to the flux distributed in the claw pole teeth is 3D, the SMC is considered to manufacture the claw pole teeth, while the flux distributed in the stator yoke is 1D and its structure is simple for production, therefore the silicon sheet or amorphous alloy is considered to be used for manufacturing the stator yoke. Fig. 4(b) shows the detail structure of its stator yoke, which is made by silicon sheets that stacked in the radial direction or rolled by amorphous alloy. Fig. 4(c) shows the claw pole teeth made by SMC which will be installed on the stator yoke. By developing the stator with hybrid cores, the PMCPM with hybrid cores has following advantages. Firstly, the mechanical strength of PMCPM can be improved. Secondly, when one claw pole teeth

are broken then machine can be repaired by replacing one claw pole teeth. Thirdly, it makes the PMCPM has the potential for developing large direct drive machine, as the compacting process of single stator teeth is much simpler.

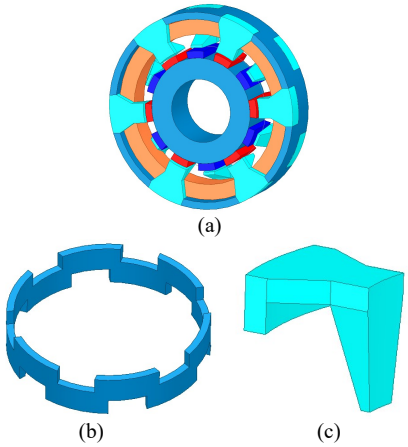

Fig. 4. (a) Schematic diagram of the structure of the PMCPM with hybrid cores. (b) silicon/AAM stator yoke. (c) SMC claw pole teeth.

III. Performance Comparison among SMC-CPM, Si-SMC-CPM and AAM-SMC-CPM

A. Main Parameters Determination

As the permeability of silicon sheet and amorphous alloy is much higher than that of SMC cores, the torque ability of Si-SMC-CPM and AAM-SMC-CPM are better than that of SMC-CPM. For verifying the performance improvement fairly, the main dimensions of these machines are optimized and their main performance are compared based on the 3D FEM. Keeping the comparison results fairly, the main dimensions of these three machines kept similarity. In the Hybrid-CPM, the main part that needs further optimization is the size of the joint of the hybrid core. Fig. 5 shows two main parameters of the joint of the Hybrid-CPM which include the stator claw pole wall width angle A1, and the joint axial length of stator claw pole wall between stator yoke Hcw.

Fig. 6(a) and (b) shows the average torque of Si-SMC-CPM and AAM-SMC-CPM with A1 and Hcw varied when the current density equals about 6 A/mm^2. As shown, when the A1 equals 24 deg and Hcw equals 7 mm, the average torque of these two machines can be maximized. The main structural parameters of the PMCPM as shown in Table II.

TABLE II
MAIN PARAMETERS OF PMCPM

Symbol	Description	Value
R_{so}	Stator outer radius	42 mm
R_{si}	Stator inner radius	26.5 mm
H_{sy}	Stator yoke thickness	3 mm
L_{gap}	Air gap length	1 mm
H_{pm}	PM thickness	3 mm
R_{ro}	Rotor outer radius	25.5 mm
R_{ri}	Rotor inner radius	13.5 mm
L_c	Axial length of claw pole teeth	16 mm
L_{all}	Axial length of one phase	18.2 mm
N_{coil}	Winding turns per phase	25
N	Pole pairs number	6

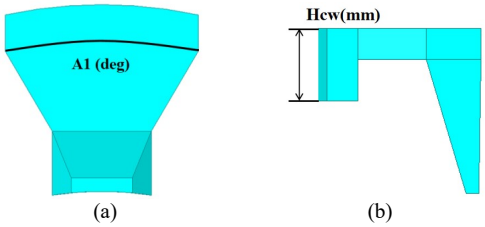

Fig. 5. (a) Stator claw pole wall width angle A1. (b) Joint axial length Hcw of stator claw pole wall between stator yoke.

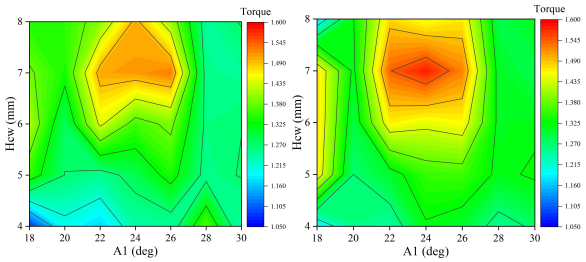

Fig. 6. Torque against with A1 and Hcw. (a) AAM-SMC-CPM. (b) Si-SMC-CPM.

B. Magnetic Flux Density Distribution Comparison

Fig. 7 shows the no load flux density distribution on these machines. As shown, the no load flux density distribution on these machines is almost similar, and the flux density on the joint part between the claw pole teeth and claw pole wall is higher than that on other parts. To compare the flux density directly, the flux density on four typical points shown in Fig. 8 are calculated, in which point 1 is located on stator yoke made by SMC, silicon sheets or amorphous alloy, point 2 is located on stator yoke joint part made by SMC, point 3 is located on claw pole wall and the point 4 is located on the stator claw pole teeth.

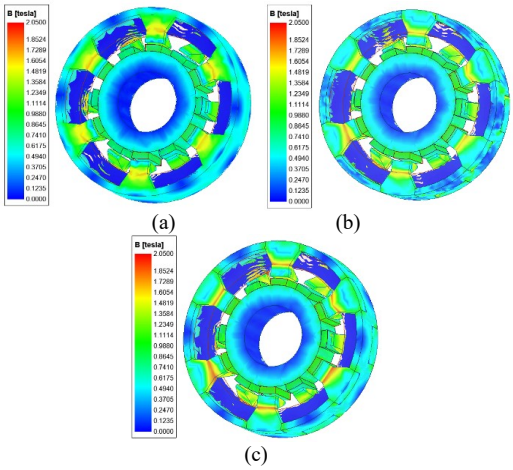

Fig. 7. No load flux density distribution. (a) SMC-CPM. (b) AAM-SMC-CPM. (c) Si-SMC-CPM.

Fig. 9 shows the flux density on above typical points versus the rotor position comparison. It can be seen that compared with SMC-CPM, the stator yoke flux density of Si-SMC-CPM is higher since the permeability of silicon sheet is higher than that of SMC. Meanwhile as the saturation flux density and stacking factor of amorphous alloy is lower than silicon sheets, the stator yoke flux density in AAM-SMC-CPM is the lowest one. While as the stator claw pole teeth of these machines are

all made by SMC, the flux density on their stator claw pole teeth is quite similar as shown in Fig. 9(c) and (d).

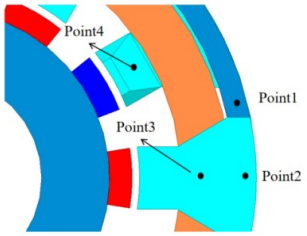

Fig. 8. Typical points in Hybrid-CPM.

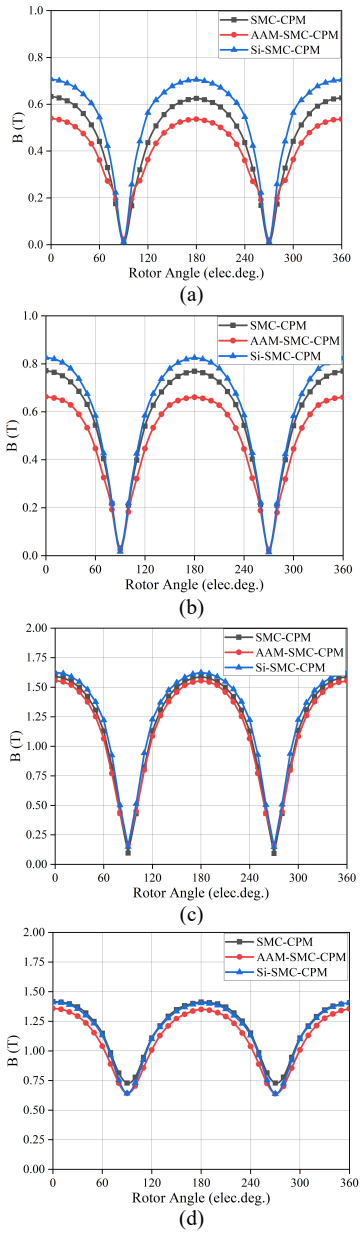

Fig. 9. Flux density versus rotor position comparison. (a) point 1. (b) point 2. (c) point 3. (d) point 4.

C. Torque Ability, Back EMF and Power Factor Comparison

Fig. 10 compares the average torque of these machines versus the current density. It can be seen that the torque ability of Si-SMC-CPM is the highest one, then the AAM-SMC-CPM, and SMC-CPM is the lowest one. Fig. 11 shows the torque waveform when the current density is 6 A/mm^2. As shown, the average torque of Si-SMC-CPM, AAM-SMC-CPM and SMC-CPM are 1.58 Nm, 1.46 Nm and 1.36 Nm respectively. Compared with SMC-CPM, the average torque of Si-SMC-CPM and AAM-SMC-CPM has been improved about 17% and 8.1% respectively, as the permeability of silicon sheet and amorphous alloy are higher and the flux saturation of amorphous alloy is lower than that of silicon sheet. Fig. 12 shows the back EMF comparison of these machines. As shown, their back EMF are almost similar.

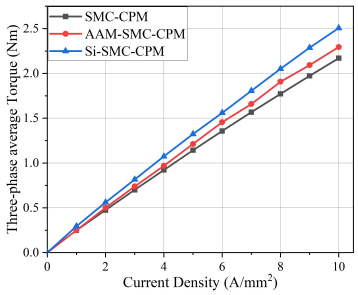

Fig. 10. Average torque comparison.

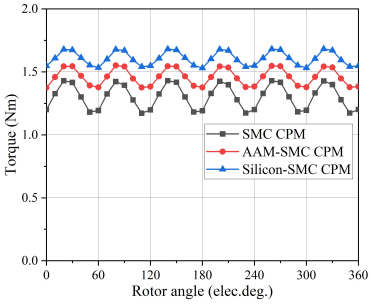

Fig. 11. Torque waveform comparison.

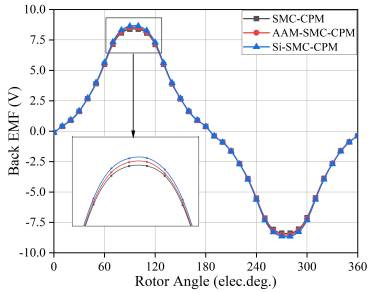

Fig. 12. No load back EMF comparison.

Fig. 13 compares the calculated power factor versus the current density of these machines. As shown, the power factor of SMC-CPM, Si-SMC-CPM, and AAM-SMC-CPM under the excitation current density of 6 A/mm^2 are 89.6%, 86%, and 81.8% respectively. It can be seen that the power factor decreases with the current density increases, and the power factor of SMC-CPM is highest one. The main reason is that the permeability of SMC is low and the leakage flux existed in Si-SMC-CPM and AAM-SMC-CPM are high, therefore the total inductance of SMC-CPM is lower, its power factor is higher than the other machines. Fig. 14 compares the calculated cogging torque versus the rotor position of these machines. As shown, the cogging torque of these machines are quite similar, since their stator claw pole structure are the same.

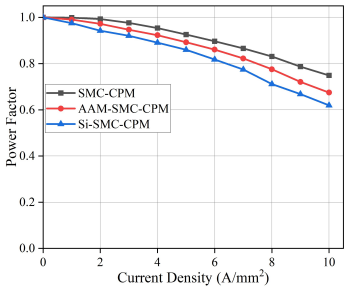

Fig. 13. Power factor comparison.

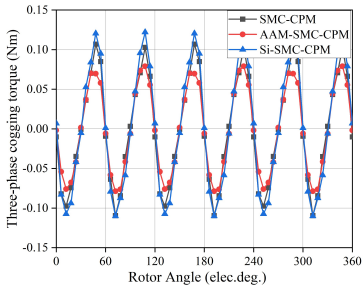

Fig. 14. Cogging torque comparison.

D. *Efficiency Comparison*

Efficiency is very important to evaluate the machine performance, which can be calculated by,

$$\eta = \frac{P_{out}}{P_{in}} = \frac{P_{em} - P_{core} - P_{mech} - P_{eddy}}{P_{em} + P_{copper}} \quad (1)$$

where P_{em} is the electromagnetic power, P_{core} is the core loss, P_{mech} is the mechanical loss, P_{eddy} is the additional eddy current loss and P_{copper} is the copper loss.

Fig. 15 compares the efficiency map of these machines. It can be seen that with employing hybrid cores the maximum efficiency of Si-SMC-CPM and AAM-SMC-CPM are decreased. However when the current density equals 6 A/mm^2, and the rotate speed equals about 1000 rpm, the efficiency of SMC-CPM, Si-SMC-CPM, and AAM-SMC-CPM are 84.9%, 85.3% and 86.2 % respectively.

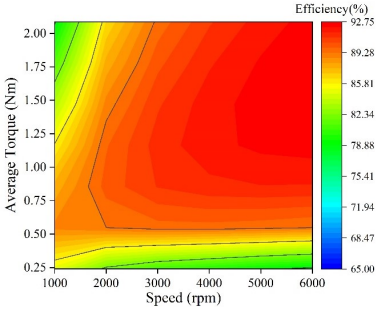

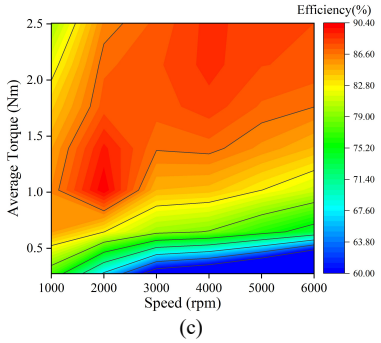

Fig. 15. Efficiency map comparison. (a) SMC-CPM. (b) AAM-SMC-CPM. (c) Si-SMC-CPM.

The main reason is that when the rotate speed is not high, the core loss of these machines is lower than the copper loss. While with the hybrid cores employed, the torque ability of Si-SMC-CPM and AAM-SMC-CPM has been improved and then their efficiency are higher. However when the rotate speed is high, the additional eddy current loss resulted on the joint part between the SMC and amorphous alloy or silicon sheet increases greatly with the operation frequency increases. Meanwhile at this operation state the core loss of the SMC is much lower than that of silicon sheets, therefore the efficiency of SMC-CPM is higher.

Though the manufacturing process of SMC raw material is much easier than that of silicon sheet and amorphous alloy, the price of SMC material is high due to its manufacturing scale is quite small currently. Therefore, the stator cost of PMCPM can be reduced by replacing the stator yoke with silicon sheets or amorphous alloy. Therefore, the Hybrid-CPM can have better performance while with low costs. Furthermore, it can be developed as modular machine that used for wind generator and electric vehicle drive system.

IV. Additional Eddy Current Loss Reduction for PMCPM with Hybrid Cores

A. *Additional Eddy Current Loss Calculation*

Compared with SMC material, the eddy current loss resulted in the silicon sheets or amorphous alloy are relatively high especially when the operation frequency is high. Replacing the stator yoke with silicon sheet or amorphous alloy will bring the electrical machine with more eddy current loss. Moreover, the magnetic flux direction will be changed and the flux vertical to the silicon sheets or amorphous alloy will be resulted in the joint part between SMC and silicon sheets or amorphous alloy, and the additional eddy current loss will be resulted.

Fig. 16 shows the calculated additional eddy current loss of the Si-SMC-CPM and AAM-SMC-CPM. The gap between the SMC and silicon sheet or amorphous alloy core are approximated equals about 0.1 mm in the FEM calculation. As shown, the additional eddy current loss increases with the rotor speed increases, and the additional eddy current loss of Si-SMC-CPM is higher than that of AAM-SMC-CPM. Table III tabulates the calculated additional eddy current loss of Si-SMC-CPM and AAM-SMC-CPM when the excitation current is 6 A/mm^2 while the rotor speed varied from 1000 rpm

to 6000 rpm. It can be seen that with the rotor speed increases the additional eddy current loss will become the main part of core loss, therefore reducing the additional eddy current loss is very important. In this section, some methods are proposed and analyzed for reducing the additional eddy current loss of Si-SMC-CPM. Fig. 17 shows the FEM model of silicon sheet in the Si-SMC-CPM.

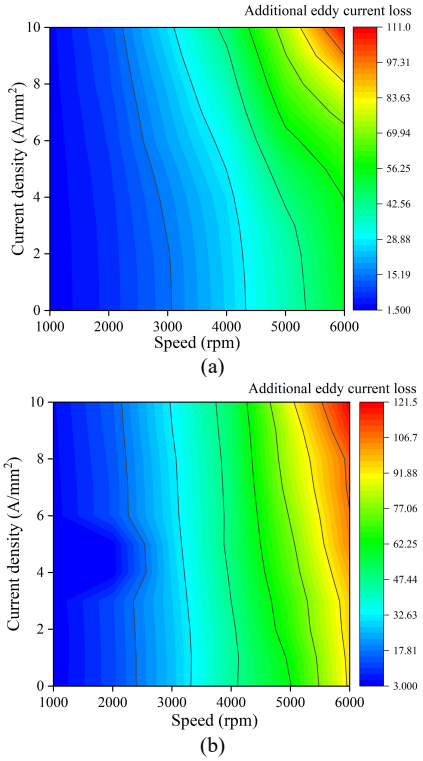

Fig. 16. Additional eddy current loss map. (a) AAM-SMC-CPM. (b) Silicon-SMC-CPM.

TABLE III
CALCULATED ADDITIONAL EDDY CURRENT LOSS COMPARISON

Speed (rpm)	AAM-SMC-CPM			Si-SMC-CPM		
	P_e (W)	P_{core} (W)	α	P_e (W)	P_{core} (W)	β
1000	2.2	4.7	0.46	3.4	7	0.48
2000	8.6	14.4	0.6	13.1	19.5	0.67
3000	19.9	29.1	0.68	29.1	40.2	0.72
4000	31.2	44.1	0.71	50.7	68.4	0.67
5000	53.4	70.5	0.76	78	102	0.76
6000	64.8	87.3	0.74	112	134.7	0.8

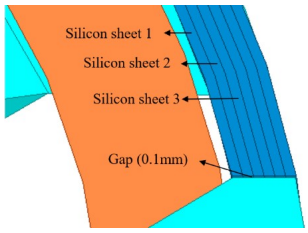

Fig. 17. Schematic diagram of silicon sheet core.

Fig. 18 shows the eddy current loss distributed on the silicon sheets when the Si-SMC-CPM operated under 5000 rpm and 6 A/mm^2. As shown, the eddy current loss is mainly distributed on the inner silicon sheets, and it is very high on the joint corner part.

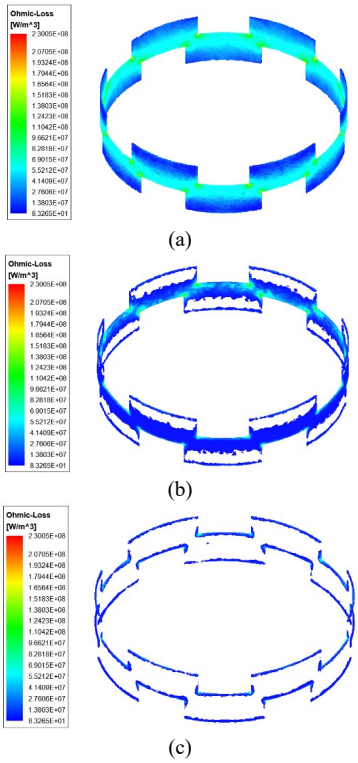

Fig. 18. Additional eddy current loss distribution. (a) silicon sheet 1. (b) silicon sheet 2. (c) silicon sheet 3.

B. Additional Eddy Current Reduction

Considering the resulted additional eddy current loss can bring the machine with high temperature rise, then the machine even can be damaged. Therefore, some methods are proposed to reduce the resulted additional eddy current loss, which include changing the joint part shape by designing the yoke part of stator claw pole teeth with a triangle with the side length of H1, adding the gap length of H2 between the winding and inner silicon sheets, and cutting some notches (notch depth of H3 and notch width of H4) on the joint part as shown in Fig. 19.

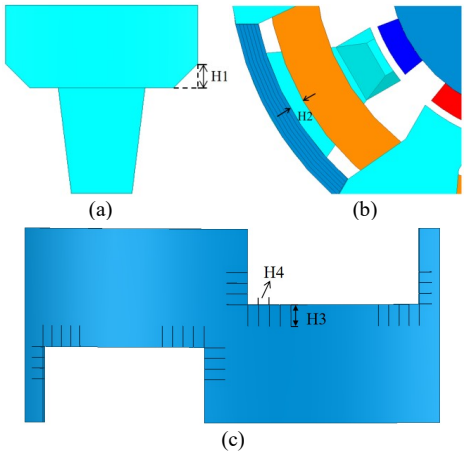

Fig. 19. Schematic diagram of structural optimization parameters. (a) H1. (b) H2. (c) H3 and H4.

By changing the shape of joint part, the magnetic flux penetrating from SMC stator claw pole teeth to silicon sheet yoke will be changed as the right angle has been canceled and the additional eddy current loss can be reduced. Fig. 20 shows the additional eddy current loss versus H1 at 5000 rpm and 6

A/mm^2. It can be seen that the additional eddy current loss decreases firstly then increases with H1 increases, and it can achieve the minimum value of 72.9 W when H1 equals about 1 mm. Fig. 20(b) shows the additional eddy current loss versus the rotor speed at 6 A/mm^2 when H1 equals about 0 mm and 1 mm. As shown, when the operation frequency is low, their difference is small, while when the operation frequency is high the additional eddy current loss can be decreased obviously.

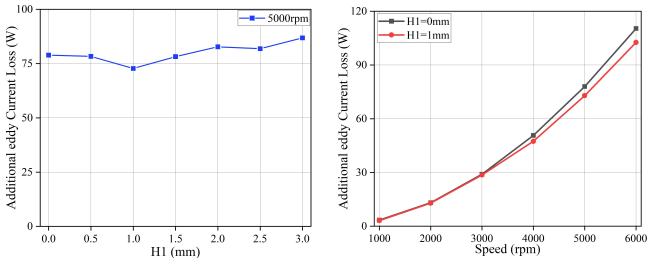

Fig. 20. (a) Additional eddy current loss versus H1. (b) additional eddy current loss versus the rotor speed.

The additional eddy current loss resulted by the main magnetic flux produced by PM and the armature magnetic flux produced by winding. With H2 increases the eddy current loss produced by the armature winding will be decreased. For making the average torque independent on H2, the total sectional area of winding kept unchanged when H2 increased. Fig. 21 compares the calculated additional eddy current loss versus the H2 increased from 0.5 mm to 2 mm. It can be seen that H2 plays an important role on reducing the additional eddy current loss especially when the rotor speed is high. When the rotor speed equals 5000 rpm and 6000 rpm, the additional eddy current loss reduced from 76.2 W to 67.8 W and 115.8 W to 96 W and the reduction ratio are 11% and 17 % respectively.

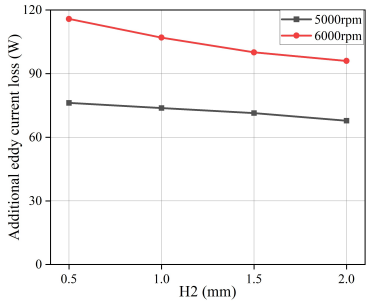

Fig. 21. Additional eddy current loss versus H2 at different speed.

As shown in Fig. 18, the additional eddy current loss concentrates on the corner part of silicon sheets core. Increasing the eddy current path is an effective way to reduce the additional eddy current loss. Fig. 22 compares the additional current loss versus the H3 and H4 when the rotor speed equals 5000 rpm. It can be seen that the additional eddy current loss decreases with H3 and H4 increases. Fig. 24 shows the additional eddy current loss density on the point 1 and point shown in Fig. 23. As shown, the additional eddy current loss density on point 1 reduced greatly with H3 increases, while the eddy current loss on point 2 kept almost unchanged. Fig. 25 shows the efficiency map of Si-SMC-CPM with notching at the joint part of SMC claw pole and silicon sheet stator yoke. As shown, the maximum operating efficiency is increased, and the high operating efficiency areas of this machine increase significantly as well.

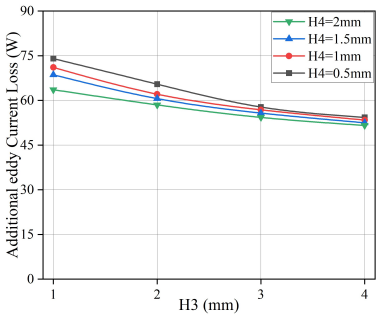

Fig. 22. Additional eddy current loss versus H3 and H4.

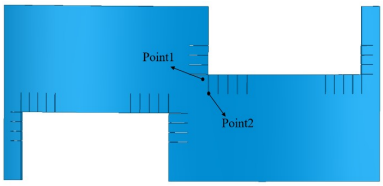

Fig. 23. Point position of laminated slotting model.

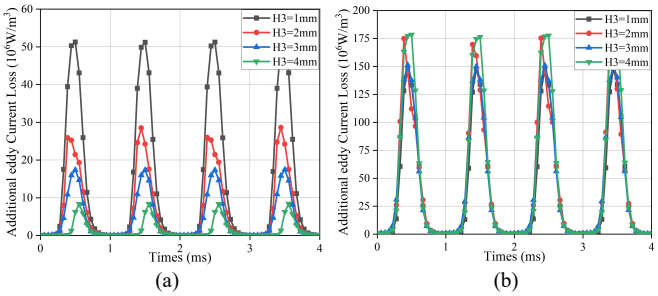

Fig. 24. Additional eddy current loss density against H3 at different positions. (a) point 1. (b) point 2.

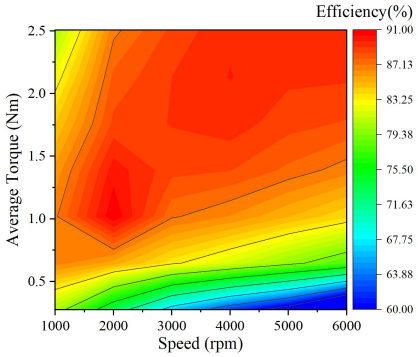

Fig. 25. Efficiency map of Si-SMC-CPM with notching at the joint part.

For comparing the performance of the Si-SMC-CPM employing above additional eddy current loss reduction methods fairly, both the torque ability and efficiency of these machines are compared. For the simplicity, they are named as Motor A, Motor B and motor C. Specifically, the H1 in motor A equals 1 mm, the H2 in motor B equals 2 mm, and H3 and H4 in Motor C equals 3 mm and 1 mm respectively. The main performance of these machines is tabulated in Table IV, when they are operated with 5000 rpm and 6 A/mm^2. As shown, with above methods employed the eddy current loss in Si-SMC-CPM can be reduced greatly and then the operation efficiency can be improved with the torque ability kept almost unchanged.

TABLE IV
PERFORMANCE COMPARISON OF SI-SMC-CPM WITH DIFFERENT ADDITIONAL EDDY CURRENT LOSS REDUCTION METHODS EMPLOYED

	Initial Si-SMC-CPM	Motor A	Motor B	Motor C
Torque (Nm)	1.58	1.58	1.57	1.58
Back EMF (V)	36.3	36.1	36.2	36.1
Additional eddy current loss (W)	78	72.9	67.8	55.5
Efficiency	85%	85.6%	86.3%	87.7%

V. CONCLUSION

A new PMCPM with hybrid silicon sheet - SMC cores and hybrid amorphous alloy - SMC cores are proposed in this paper. Compared with PMCPM with SMC cores, the PMCPM with hybrid cores can have higher efficiency for low-speed operation and higher torque ability. On the other hand, the proposed PMCPM with hybrid cores has lower power factor and lower efficiency for high-speed operation when compared with PMCPM with SMC cores. The main reason is that the additional eddy current loss is resulted in the joint part of hybrid core in the Hybrid-CPM. Therefore three methods to reduce this kind of eddy current loss are proposed in this paper. It can be seen that with corresponding methods employed the efficiency of PMCPM with hybrid cores can be improved greatly. Compared with PMCPM with SMC cores, the PMCPM can have the merits of low cost, high torque ability, more wide high efficiency operation range.

REFERENCES

[1] Y. Zhang, R. Qu, D. Li, Y. Cheng, Y. Gao, and Q. Wang, "Design and Optimization of an HTS Claw-Pole Machine," *IEEE Trans. Appl. Supercond.*, vol. 30, no. 4, pp. 1-6, June 2020.

[2] Y. Zhang, D. Li, P. Yan, X. Ren, R. Qu and J. Ma, "A High Torque Density Claw-Pole Permanent-Magnets Vernier Machine," *IEEE Journal of Emerging and Selected Topics in Power Electronics*, vol. 10, no. 2, pp. 1756-1765, April 2022.

[3] C. Liu et al., "Performance Evaluation of an Axial Flux Claw Pole Machine With Soft Magnetic Composite Cores," *IEEE Trans. Appl. Supercond.*, vol. 28, no. 3, pp. 1-5, April 2018.

[4] A. Schoppa, and P. Delarbre, "Soft Magnetic Powder Composites and Potential Applications in Modern Electric Machines and Devices," *IEEE Trans. Magn.*, vol. 50, no. 4, pp. 1-4, April 2014.

[5] C. Liu, G. Lei, T. Wang, Y. Guo, Y. Wang, and J. Zhu, "Comparative Study of Small Electrical Machines with Soft Magnetic Composite Cores," *IEEE Trans. Ind. Electron.*, vol. 64, no. 2, pp. 1049-1060, Feb. 2017.

[6] C. C. Liu, D. Y. Wang, S. P. Wang, and Y. H. Wang, "A Novel Flux Reversal Claw Pole Machine With Soft Magnetic Composite Cores," *IEEE Trans. Appl. Supercond.*, vol. 30, no. 4, pp. 1-5, June 2020.

[7] L. Rabenstein, A. Dietz, and N. Parspour, "Design Concept of a Wound Field Transverse Flux Machine using Soft Magnetic Composite Claw-Poles," in *Proc. of 2020 10th International Electric Drives Production Conference (EDPC)*, Ludwigsburg, Germany, 2020, pp. 1-5.

[8] A. Krings, A. Boglietti, A. Cavagnino, and S. Sprague, "Soft Magnetic Material Status and Trends in Electric Machines," *IEEE Trans. Appl. Supercond.*, vol. 64, no. 3, pp. 2405-2414, March 2017.

[9] B. Scheerlinck, H. De Gersem, and P. Sergeant, "3-D Eddy Current and Fringing-Flux Distribution in an Axial-Flux Permanent-Magnet Synchronous Machine With Stator in Laminated Iron or SMC," *IEEE Trans. Magn.*, vol. 51, no. 11, pp. 1-4, Nov. 2015.

[10] A. Schoppa and P. Delarbre, "Soft Magnetic Powder Composites and Potential Applications in Modern Electric Machines and Devices," *IEEE Trans. Magn.*, vol. 50, no. 4, pp. 1-4, April 2014.

[11] D. P. Morisco, I. L. Iepure, and A. Moeckel, "Enhanced 3D finite element method analysis of a permanent magnet machine with reduced stator-core iron losses," in *Proc. of 2017 IEEE International Electric Machines and Drives Conference (IEMDC)*, Miami, Florida, USA, 2017, pp. 1-7.

[12] S. Wang, C. Liu, Y. Wang, G. Lei, Y. Guo, and J. Zhu, "Electromagnetic performance analysis of flux-switching permanent magnet tubular machine with hybrid cores," *CES Transactions on Electrical Machines and Systems*, vol. 4, no. 1, pp. 43-52, March 2020.

[13] W. Zhang, Y. Xu, and M. Sun, "Design of a Novel Claw Pole Transverse Flux Permanent Magnet Motor Based on Hybrid Stator Core," *IEEE Trans. Magn.*, vol. 57, no. 6, pp. 1-5, June 2021.

[14] Z. Wang, Y. Enomoto, R. Masaki, K. Souma, H. Itabashi, and S. Tanigawa, "Development of a high speed motor using amorphous metal cores," in *Proc. of 8th International Conference on Power Electronics - ECCE Asia*, Jeju, Korea (South), 2011, pp. 1940-1945.

[15] W. Tong, S. Dai, S. Wu, and R. Tang, "Performance Comparison between an Amorphous Metal PMSM and a Silicon Steel PMSM," *IEEE Trans. Magn.*, vol. 55, no. 6, pp. 1-5, June 2019.

[16] M. M. Zaid, H. Ahmad, I. Sami, A. Waheed, S. S. Hussain Bukhari, and J. -S. Ro, "Design of a High Torque Density Interior Permanent Magnet Synchronous Machine with improved Efficiency using Amorphous Magnetic Material," in *Proc. of 2021 IEEE International Magnetic Conference (INTERMAG)*, LYON, France, 2021, pp. 1-4.

Chengcheng Liu (S'14 – M'16) was born in Jiangsu, China in 1988. He received the B.E. degree in automation engineering from Yangzhou University, Yangzhou, China, in 2010 and the Ph.D. degree in electrical engineering from Hebei University of Technology, Tianjin, China, in 2016. He was a joint Ph.D. student supported by the Chinese scholarship council in the University of Technology, Sydney, Australia.

He is currently an associate professor at Hebei University of Technology, Tianjin, China. His research interests include the design, analysis and optimization of electromagnetic devices.

Zheng Chao was born in China on January 1999. He received the B.E. degree in electrical engineering from Shandong University of Technology, Zibo, China, in 2020. He is currently pursuing the M.E. degree in electrical engineering at Hebei University of Technology, Tianjin, China. His current research interests include design and optimization of electromagnetic devices.

Shaopeng Wang was born in Hebei, China, in 1993. He received the B.E. degree and M.E. degree in Electrical Engineering from Hebei University of Technology, Tianjin, China, in 2016 and 2019, where he is currently working toward the Ph.D. degree in electrical engineering from Hebei University of Technology

His current research interests include design and optimization of electromagnetic devices.

Youhua Wang received the B.E. degree from Xian Jiaotong University, Xian, China, in 1987; the M.E. degree from the Hebei University of Technology, Tianjin, China, in 1990; and the Ph.D. from Fuzhou University, Fuzhou, China, in 1994, all in electrical apparatus.

He is currently a Professor at the College of Electrical Engineering. His current research interests include measurement and modeling of properties of magnetic materials, numerical analysis of the electromagnetic field, and electromagnetic device design, analysis and optimization.